ENERGY EFFICIENT DRIVE OF AN OMNIDIRECTIONAL MOBILE ROBOT WITH STEERABLE OMNIDIRECTIONAL WHEELS

Jae-Bok Song, Jeong-Keun Kim

Department of Mechanical Engineering, Korea University, Seoul, Korea
(Tel : +82-2-3290-3363 ; E-mail: jbsong@korea.ac.kr)

Abstract: In this paper the second version of the omnidirectional mobile robot with steerable omnidirectional wheels (OMR-SOW) is presented. This robot can operate in either the omnidirectional or the differential drive mode depending on the drive conditions. In the omnidirectional mode, it has 3 DOFs in motion and 1 DOF in steering which can function as a continuously-variable transmission (CVT). The CVT function can be used to enhance energy efficiency of the robot operation by increasing the range of velocity ratio of the robot velocity to wheel velocity. Kinematics and dynamics of this robot are examined. In the proposed steering algorithm, the steering angle is controlled so that motors may operate in the region of high velocity and low torque, thus generating the maximum energy efficiency. Various tests show that motion control of the OMR-SOW works satisfactorily and the proposed steering algorithm for CVT can provide higher energy efficiency than the algorithm using a fixed steering angle. In addition, it is shown that the differential drive mode can give better energy efficiency the omnidirectional drive mode.

Keywords: Omnidirectional mobile robot, Energy efficient drive, Continuously-variable transmission (CVT), Steering algorithm.

1. INTRODUCTION

Applications of wheeled mobile robots have recently extended to the service robots for the handicapped or the aged and the industrial mobile robots working in various environments. The most popular wheeled mobile robots are equipped with two independent driving wheels. Since these robots possess 2 degrees-of-freedom (DOFs), they can rotate about any point, but cannot perform sideways motion. To overcome this type of limitation on motion, omnidirectional mobile robots (OMRs) were proposed. They are capable of moving in an arbitrary direction without changing the direction of wheels, because they can achieve 3 DOF motion on a 2-dimensional plane. Various types of omnidirectional mobile robots have been proposed so far: universal wheels (Blumrich, 1974) ball wheels (West and Asada, 1997) are popular among them.

The OMRs using omnidirectional wheels composed of passive rollers or balls usually have 3 or 4 wheels. It is desirable that four-wheeled vehicles be used when stability is of great concern (Muir and Neuman, 1987). However, independent drive of four wheels creates one extra DOF. To cope with such a redundancy problem, the mechanism capable of driving four omnidirectional wheels using three actuators was suggested (Asama et al., 1996).

One approach to a redundant DOF is to devise some mechanism which uses this redundancy to change wheel arrangements (Wada and Asada, 1999). It is called a variable footprint mechanism. Since the relationship between the robot velocity and wheel velocities depends on wheel arrangement, varying wheel arrangement can function as a transmission. This mobile robot, however, has a limited range of wheel arrangement to ensure stability of the vehicle. To cope with this limitation, the Omnidirectional Mobile Robot with Steerable Omnidirectional Wheels (OMR-SOW) was proposed (Song and Byun, 2004) as shown in Fig. 1. Since the OMR-SOW extended the range of velocity ratio significantly,

stability was guaranteed regardless of wheel arrangements.

Fig. 1. Photo of omnidirectional mobile robot.

Energy efficiency is of great importance in mobile robots because it is directly related to the operating time without recharging. The OMR-SOW has a function of a continuously-variable transmission (CVT), because the robot velocity can change continuously by adjustment of wheel arrangements without employing a gear train. The CVT can provide energy efficient drive of the OMR-SOW. If the CVT is not properly controlled, however, energy-saving capability can be deteriorated. Hence, a proper control algorithm is essential to energy efficient drive. The CVT control of the OMR-SOW, however, is quite different from the automotive one in that it is related to all four motors unlike an automotive CVT (Liu and Paden, 1997). In this research, a simple and effective algorithm for control of CVT considering efficiency of motor drive is suggested and verified by various experiments.

The OMR-SOW has some drawbacks. When the omnidirectional capability is not required especially in the normal straight-line driving, the omni-directional mechanism tends to prevent the robot from driving efficiently. In this case, the wheel arrangement used in the automobile (i.e., 4 wheels in parallel) is preferred to the omnidirectional mechanism. Furthermore, the maximum height of a surmountable bump for OMR is the radius of the passive roller of the omnidirectional wheel, which is much smaller than the radius of the wheel for the ordinary mobile robot. To cope with these drawbacks, it is desirable that the robot functions as an ordinary mobile robot unless its task requires omnidirectional capability. In this research, a new mechanism is proposed which can be used as the differential drive mechanism as well as the omnidirectional one.

2. STRUCTURE & OPERATION OF OMR-SOW

2.1 *Structure of OMR-SOW*

The coordinate systems for the OMR-SOW are illustrated in Fig. 2. The frame *O-XY* is assigned as a reference frame for robot motion in the plane and the moving frame *o-xy* is attached to the robot center. The angle θ between the *y*-axis and the diagonal line of the robot body depends on the shape of a body (i.e., $\theta = 45^{o}$ for the square body). The four wheel modules can rotate about each pivot point C_1, .., C_4 located at the corners of the robot body, but they are constrained to execute a synchronized steering motion of 1 DOF by the mechanism comprising the connecting links and the linear guide. Note that steering is indirectly determined by the vector sum of each wheel velocity (not by an independent steering motor). In Fig. 2, the steering angle ϕ is defined as the angle from the zero position in which coincides with the diagonal lines (i.e., C_1C_3 or C_2C_4) of the robot body. The steering angle changes in the range of -30^{o} to $+30^{o}$ in the omnidirectional drive mode, while maintained at $+45^{o}$ or -45^{o} in the differential drive mode as shown in Fig. 3.

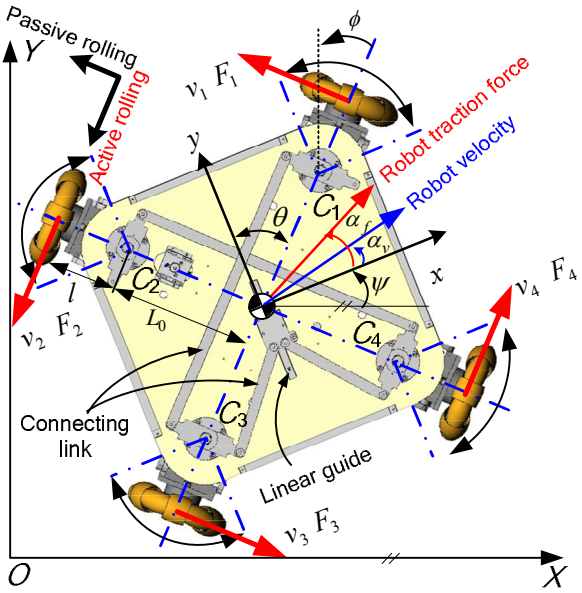

Fig. 2 Coordinate systems for OMR-SOW.

This robot contains the wheel module comprising the four omnidirectional wheels connected to individual motors, a variable wheel arrangement mechanism, and a square platform whose side is 500mm. The omnidirectional wheels used in the robot are called the *continuous alternate wheel* (CAW) developed in our laboratory, where inner and outer rollers are arranged continuously, thus resulting in no gap between the rollers as shown in Fig. 4 (Byun and Song, 2003). In the CAW, the wheel velocity can be divided into the components in the active direction and in the passive direction. The active component is directed along the axis of the roller in contact with the ground, while the passive one is perpendicular to the roller axis. These wheels are connected to the DC motors through timing belts. Wheel suspension systems are required to ensure that the wheels are in contact with the ground at all times. This suspension can also absorb the shock transmitted to the wheels.

Fig. 5 illustrates the control systems for the OMR-SOW. DSP (TMS320F2812) is used as both a master controller and motor controllers. The master controller plans the robot trajectory and gives the

commands to the motor controller where motor control is performed.

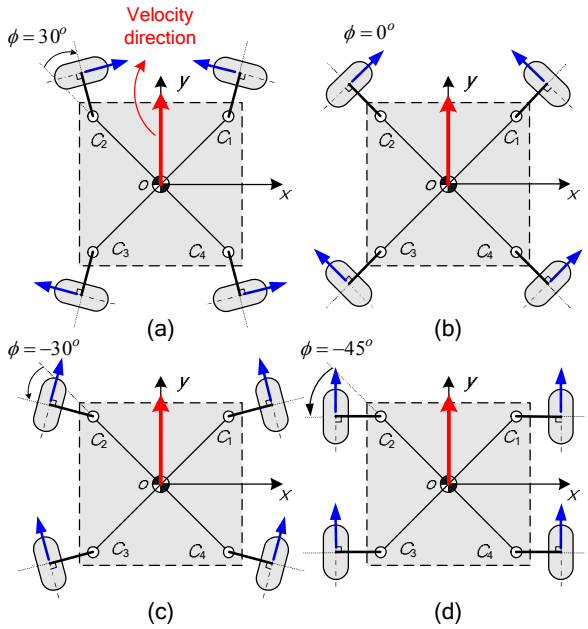

Fig. 3 Various wheel arrangements; (a) $\phi = 30°$, (b) $\phi = 0°$, (c) $\phi = -30°$, (d) $\phi = -45°$

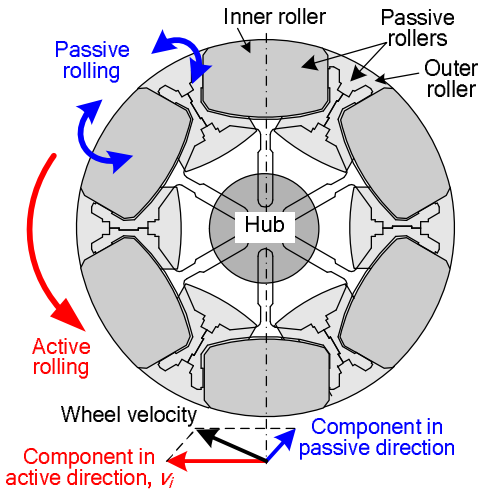

Fig. 4 Appearance of continuous alternate wheel and active and passive rolling.

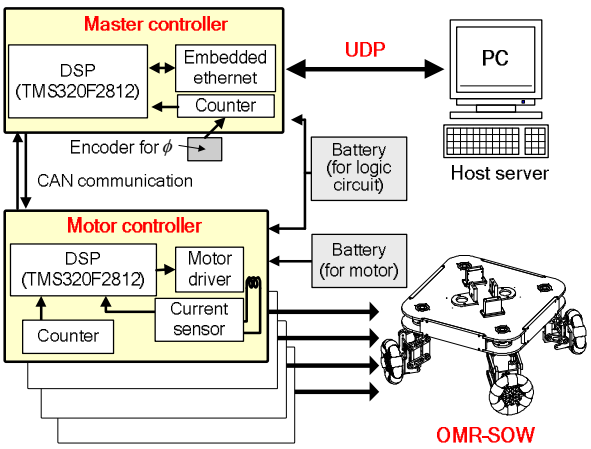

Fig. 5 Control systems for OMR-SOW

2.2 Kinematic Analysis

The relationship between the wheel velocity vector V_w and the robot velocity vector V_r is given by

$$V_w = J^{-1}V_r \text{ or } V_r = JV_w \tag{1}$$

where $V_w = [v_1 \ v_2 \ v_3 \ v_4]^T$, $V_r = [v_x \ v_y \ \dot{\psi} \ \dot{\phi}]^T$, and the Jacobian matrix is given as

$$J = \frac{1}{4}\begin{bmatrix} -1/C & -1/C & 1/C & 1/C \\ 1/S & -1/S & -1/S & 1/S \\ 1/L & 1/L & 1/L & 1/L \\ 1/l & -1/l & 1/l & -1/l \end{bmatrix}, \quad \begin{cases} C = \cos(\theta - \phi) \\ S = \sin(\theta - \phi) \\ L = L_o \cos\phi + l \end{cases} \tag{2}$$

where v_1, v_2, v_3, and v_4 are the wheel velocities in the active direction, v_x and v_y the translational velocities of the robot center, $\dot{\psi}$ the angular velocity about the robot center, and $\dot{\phi}$ the derivative of the steering angle, respectively. It follows from Eq. (1) that the robot velocity and steering velocity of the OMR-SOW can be completely determined by control of four independent motors driving each wheel. Since the omnidirectional mobile robot is of 3 DOFs in the 2-D plane, it is difficult to define the velocity ratio in terms of scalar velocities. Thus the velocity ratio is defined using the concept of norms as follows

$$r_v = \frac{\| V_r \|}{\| V_w \|} = \frac{\| JV_w \|}{\| V_w \|} \tag{3}$$

On the other hand, the force and moment of a robot can be expressed from the geometry in Fig. 2 by

$$F_r = J^{-T}F_w \text{ or } F_w = J^T F_r \tag{4}$$

where $F_w = [F_1 \ F_2 \ F_3 \ F_4]^T$, $F_r = [F_x \ F_y \ T_z \ T_\phi]^T$. F_x and F_y are the forces acting on the robot center in the x and y directions, T_z the moment about the z axis passing through the robot center, and T_ϕ the torque required to rotate the wheel modules, respectively. The force F_i (i =1,.., 4) is the traction force acting on the wheel in the direction of active rolling as shown in Fig. 2. The force ratio of the force acting on the robot center to the wheel traction force can be defined in the same way as the velocity ratio in Eq. (3) as follows

$$r_f = \frac{\| F_r \|}{\| F_w \|} = \frac{\| J^{-T}F_w \|}{\| F_w \|} \tag{5}$$

Note that the force ratio corresponds to the inverse of the velocity ratio.

3. STEERING ALGORITHM FOR CVT

In this section, a steering algorithm for CVT is discussed. The CVT of an automobile can keep the engine running within the optimal range with respect to fuel efficiency or performance. Using the engine efficiency data, the CVT controls the engine

operating points under various vehicle conditions. A CVT control algorithm for the OMR-SOW ought to include the effects of all four motors. A simple and effective algorithm for control of the CVT is proposed based on the analysis of the operating points of a motor.

3.1. Motion Control of OMR-SOW

The motion of a mobile robot can be controlled by wheel velocities. From Eq. (1), when the desired robot motion is given, the reference velocity of each wheel can be computed by

$$V_{wd} = J^{-1} V_{rd} \tag{6}$$

As shown in Fig. 6 representing the block diagram of the control system for OMR-SOW, when the velocity command $V_{wd} = [v_{1d}\ v_{2d}\ v_{3d}\ v_{4d}]^T$ is given to each motor, the PI controller performs velocity control of each motor to generate the control signal $u_i (i = 1, .., 4)$. If each wheel is controlled to follow the reference velocity, then the robot can achieve the desired motion. Practically, all mobile robots have slip between the wheels and the ground to some extent. This slip causes the real motion to be different from the desired one. Since the robot does not have any sensor measuring the robot velocity, this error is somewhat inevitable.

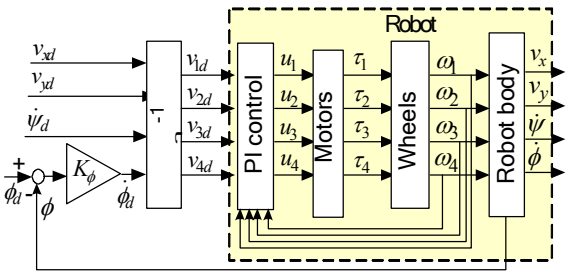

Fig. 6 Control system of OMR-SOW with steering angle control.

Since 4 wheels are independently controlled in OMR-SOW, a steering angle can be arbitrarily selected while the desired robot velocity is achieved. The desired reference steering angle ϕ_d is determined by the steering algorithm so that the maximum energy efficiency is achieved. Therefore, the desired steering velocity is computed by

$$\dot{\phi}_d = K_\phi (\phi_d - \phi) \tag{7}$$

where K_ϕ is the control gain of steering and ϕ is the actual steering angle measured by the encoder installed on the steering axis.

Fig. 7 shows operating points of a motor used in the mobile robot. In the figure T_{max} is the maximum continuous torque, ω_{max} is the maximum permissible angular velocity, the solid lines represent constant efficiency and the dashed lines denote constant output power. The input power is obtained by the product of input current and voltage and the output power is measured by the product of motor angular velocity and torque. The efficiency η is the ratio of the output to input power.

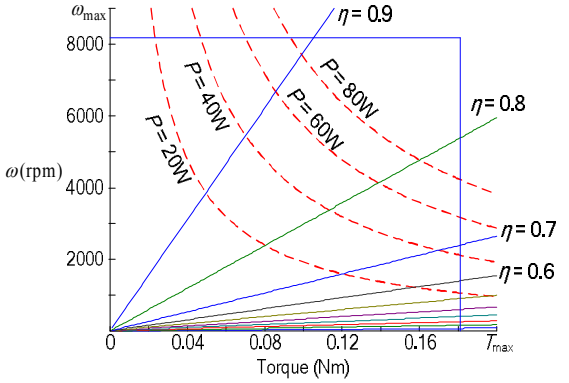

Fig. 7 Operating range of a motor.

It is shown in this figure that the efficiency varies as the operating point moves on the constant output power line. The operating point of a motor can be varied by the operation of CVT. For the same output power, a reduction in force ratio of CVT leads to a decrease in velocity and an increase in torque and then a decrease in efficiency. It is desirable, therefore, that the CVT be controlled so that motors operate in the region of high velocity and low torque.

3.2 Steering Algorithm

As explained in Section 3.1, when the desired robot velocity V_{rd} is given, independent control of each wheel is conducted to achieve it. Even for the identical robot velocity, an arbitrary steering angle can be chosen. In this section, the steering algorithm is proposed to determine the steering angle that causes the maximum energy efficiency.

In Fig. 6, velocity control is conducted by means of each motor controller. The current sensor at each motor drive measures the motor current, thereby computing the motor torque $\tau = [\tau_1\ \tau_2\ \tau_3\ \tau_4]^T$. The wheel traction force F_w can then be computed by

$$F_{wd} = (\tau - I_w \dot{\omega}_w - c_w \omega_w)/r \tag{8}$$

where r is the wheel radius, I_w is the moment of inertia of the wheel about the wheel axis and c_w is the viscous friction factor of the wheel, and $\omega_w = [\omega_1\ \omega_2\ \omega_3\ \omega_4]^T$ is the wheel angular velocity. By substituting (8) into (4), the robot traction force F_r can be obtained, thus leading to the robot traction force angle α_f measured from the x axis.

Figure 8 shows the force ration r_f defined in (5) in terms of the robot traction force angle α_f and the steering angle ϕ. It is seen that identical wheel traction forces can generate substantially different robot traction forces depending on α_f and ϕ. As explained in Section 3.1, OMR-SOW capable of CVT has the maximum energy efficiency in the region with highest force ratio (i.e., high speed and low torque). For example, when $\alpha_f = 90°$, the

steering angle of -30° can generate maximum energy efficiency. In conclusion, if the CVT is controlled in consideration of the steering pattern for each driving condition, the energy efficient driving is achieved.

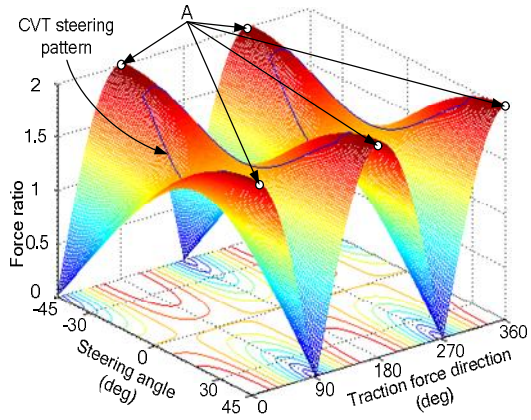

Fig. 8 Force ratio as a function of steering angle and force direction.

If the steering angle ϕ is set to either +45° or -45°as shown in Fig. 3(d), the OMR-SOW can be driven in the differential drive mode. In this mode, the OMR-SOW has the maximum force ratio denoted as A as shown in Fig. 8, thus leading to the higher energy efficiency than the omnidirectional drive mode. However, the change from the omnidirectional to the differential drive mode cannot be made while the robot is moving, because the steering angle greater than ±30° brings about slip between the wheel and ground, and passive rollers cannot be controlled. Hence, the robot should stop temporarily to conduct this conversion.

4. EXPERIMENTS

Various tests have been conducted to demonstrate performance of the constructed omnidirectional mobile robot with CVT function. Fig. 9 shows the tracking performance of OMR-SOW for a circular trajectory. This tracking was associated with both translational and rotational motion. In the experiment, the robot moved in the x-direction and simultaneously rotated about the z-axis. It is seen that the actual trajectory represented in the solid line tracked the reference reasonably relatively well. Some error was observed around the finish, since the prototype vehicle did not implement any position control algorithm for this test and thus the position error was accumulated during motion.

Energy consumption according to the wheel arrangement was investigated. The robot travelled at a speed of 0.05m/s in the y-axis in Fig. 3. This motion could be achieved in various wheel arrangements. Among them, 4 configurations were chosen including 3 omnidirectional drive modes and 1 differential drive mode (see Fig. 3). The experimental results are summarized in Table 1. As expected, the differential drive provided better energy efficiency than the omnidirectional drives. This result justifies the proposed mechanism capable of conversion between the omnidirectional and the differential drive mode depending on the drive conditions.

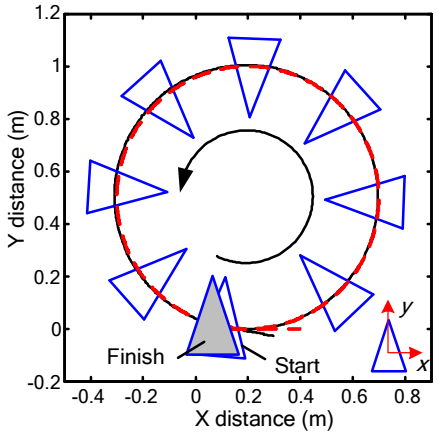

Fig. 9 Experimental results of tracking performance for a circular trajectory. (solid line: actual trajectory, dashed line: reference trajectory)

Table 1 Comparison of omnidirectional drive with differential drive

Experiments	ϕ	Average current (A)	Power (W)	Energy (J)
(a)	30	0.385	9.246	924.6
(b)	0	0.296	7.112	711.2
(c)	-30	0.275	6.605	660.5
(d)	-45	0.266	6.402	640.3

A series of experiments using a fixed steering angle and a steering angle computed by the proposed steering algorithm have been conducted. In Fig. 10, the robot followed a 1.2m x 1.2m square trajectory at a speed of 0.05m/s. Fig. 10(a) showed the result using a fixed steering angle and the consumed energy was measured as 221.3J. In Fig. 10(b), the steering angle was chosen by the force direction computed using measured currents by Eq. (18) and Fig. 8. The energy values for these experiments were measured as 179.5J. It was shown that the consumed energy was reduced 15% by the proposed steering algorithm.

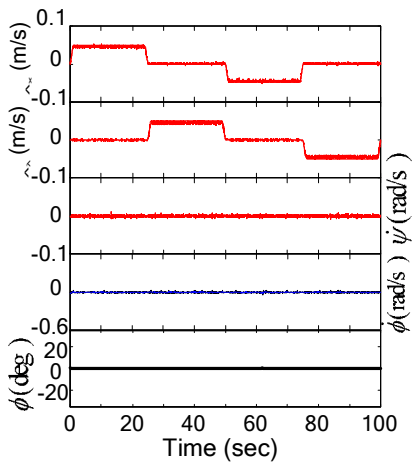

(a) Fixed steering angle

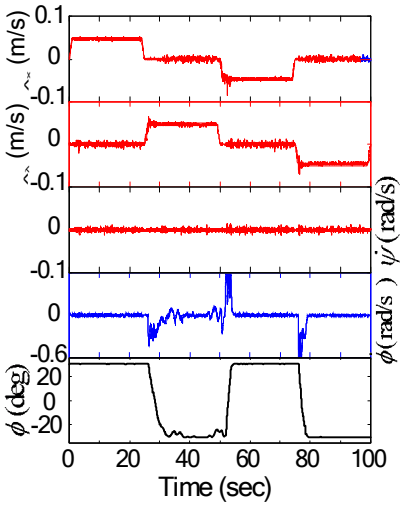

(b) Variable steering angle by steering algorithm

Fig. 10 Experimental results for square trajectory

If a ramp exists on the path as shown in Fig. 11, the measured currents change to follow the desired motion of a robot. The measured currents indirectly reflect information on the conditions of the ground or disturbance. Even for a ramp or disturbance, therefore, the steering algorithm based on the measured current can select proper steering angles. The consumed energy was reduced 14% and measured as 653.4J. Table 2 summarizes experimental results.

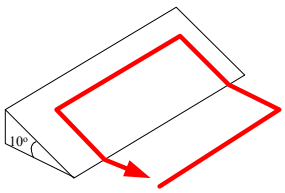

Fig. 11 Square trajectory with ramp

Table 2 Summary of experimental results with and without steering algorithm

	Square trajectory	Square trajectory with ramp
Fixed steering	221.3J	765.7J
Steering algorithm	179.5J (-15%)	635.4J (-14%)

The conventional wheels used in automobiles usually show better performance than the omnidirectional wheels with passive rollers. This is because the height of a surmountable bump for the omnidirectional wheels is limited by the radius of the smallest passive roller and the friction force of the roller. Thus if the passive rollers are constrained not to rotate as in the differential drive mode, even the omnidirectional wheels can function as the conventional ones. The omnidirectional wheel goes over a 5cm high bump which is greater than the radius of the passive roller.

5. CONCLUSIONS

In this research, an omnidirectional mobile robot with steerable omnidirectional wheels (OMR-SOW) was proposed. The kinematic and dynamic analysis was presented. From this research, the following conclusions are drawn:

1. The proposed steering algorithm for CVT can provide a significant reduction in driving energy than the algorithm using a fixed steering angle. Therefore, the size of an actuator to meet the specified performance can be reduced or performance of the mobile robot such as gradability can be enhanced for given actuators.
2. Energy efficiency can be further improved by selecting the differential drive mode by adjusting the wheel arrangement of OMR-SOW.
3. The height of the surmountable bump in the differential drive mode is much larger than that in the omnidirectional drive mode.

ACKNOWLEDGEMENTS

This work was supported by grant No. (R01-2003-000-10336-0) from the Basic Research Program of the Korea Science & Engineering Foundation.

REFERENCES

Asama, H., M. Sato, N. Goto, A. Matsumoto, I. Endo (1996). Mutual transportation of cooperative mobile robots using forklift mechanisms. *Proc. of Int. Conf. on Robotics and Automation*, pp.1754-1759.

Blumrich, J.F. (1974). "Omnidirectional vehicle," United States Patent 3,789,947.

Byun, K.-S., J.-B. Song (2003). Design and Construction of Continuous Alternate Wheels for an Omni-Directional Mobile Robot. *Journal of Robotic Systems*, **20**(9), pp. 569-579.

Liu, S., B. Paden (1997). A survey of today's CVT controls. *Proc. of the 36th conference on decision & control*, pp. 4738-4743.

Muir, P., and C. Neuman. (1987). Kinematic modeling of wheeled mobile robots. *Journal of Robotic Systems*, **4**(2), pp. 281-340.

Song, J.-B., K.-S. Byun (2004). Design and Control of an Omnidirectional Mobile Robot with Steerable Omnidirectional Wheels. *Journal of Robotic Systems*, **21**(4), pp. 193-208.

Wada, M., H. Asada (1999). Design and control of a variable footprint mechanism for holonomic omnidirectional vehicles and its application to wheelchairs. *IEEE Trans. on Robotics and Automation*, **15**(6), pp. 978-989.

West. M., H. Asada (1997). Design of ball wheel mechanisms for omnidirectional vehicles with full mobility and invariant kinematics. *Journal of Mechanical Design*. **119**, pp. 153-161.